

Magnetic-resonance study of the diluted magnetic semiconductor $\text{Pb}_{1-x-y}\text{Sn}_y\text{Mn}_x\text{Te}$

T. Story,* P. J. T. Eggenkamp, C. H. W. Swüste, H. J. M. Swagten, and W. J. M. de Jonge
Department of Physics, Eindhoven University of Technology, P.O. Box 513, 5600 MB Eindhoven, The Netherlands

A. Szczerbakow

Institute of Physics, Polish Academy of Sciences, Al. Lotników 32/46, 02-668 Warsaw, Poland

(Received 20 July 1992)

Electron paramagnetic resonance (EPR) was investigated in samples of the magnetically diluted semiconductor $\text{Pb}_{1-x-y}\text{Sn}_y\text{Mn}_x\text{Te}$ in the temperature range $T=1.3\text{--}100\text{ K}$. The samples had compositions in the range $x=0.005\text{--}0.06, y=0.12\text{--}0.72$ and carrier concentrations between $p=1.6\times 10^{19}$ and $1.4\times 10^{21}\text{ cm}^{-3}$. The temperature dependence of the EPR linewidth is strongly dependent on the carrier concentration. This can be understood within the framework of the Korringa relaxation mechanism and the two-valence-band model of magnetic properties of these crystals. For samples with high carrier concentrations (ferromagnetic at low temperatures) we obtained an s - d exchange integral of $J_{sd}=33\pm 2\text{ meV}$. The role of metal vacancies in the effect of electron bottleneck of the EPR is also discussed.

I. INTRODUCTION

In this paper we will present results of electron paramagnetic resonance (EPR) experiments in the diluted magnetic (semimagnetic) semiconductor $\text{Pb}_{1-x-y}\text{Sn}_y\text{Mn}_x\text{Te}$.¹ $\text{Pb}_{1-x-y}\text{Sn}_y\text{Mn}_x\text{Te}$ crystals can be grown within the full range of matrix compositions ($y=0\text{--}1$),² while, depending on the composition of the matrix, homogeneous crystals can be obtained up to about $x=0.1\text{--}0.3$. Manganese substitutes Pb^{2+} or Sn^{2+} ions in the metal sublattice of the rock salt crystal lattice of the host material, is electrically inactive and does not qualitatively influence the electron properties of the alloy. Typical carrier concentrations are large ($p=10^{19}\text{--}10^{21}\text{ cm}^{-3}$) and do not depend on temperature. Carriers are generated due to vacancies in the metal sublattice.² The number of carriers can be controlled by thermal annealing. $\text{Pb}_{1-x-y}\text{Sn}_y\text{Mn}_x\text{Te}$ crystals are narrow gap semiconductors with a direct energy gap at the L point of the Brillouin zone. In p -type crystals with a very high concentration of carriers ($p > p_t = 3 \times 10^{20}\text{ cm}^{-3}$) the second valence band of heavy holes is also populated [Fig. 1(a)]. Due to the large difference in the effective mass of carriers in these two bands, there is a direct effect both on electronic and magnetic properties of $\text{Pb}_{1-x-y}\text{Sn}_y\text{Mn}_x\text{Te}$.

The experimental studies of magnetic properties of the crystals of $\text{Pb}_{1-x-y}\text{Sn}_y\text{Mn}_x\text{Te}$ revealed very interesting phenomena. In samples with carrier concentrations $p > 3 \times 10^{20}\text{ cm}^{-3}$ a ferromagnetic phase is observed at helium temperatures as experimentally evidenced in magnetization, magnetic susceptibility, specific-heat,³⁻⁶ EPR,⁷ and neutron-diffraction measurements.⁸ In crystals with a carrier concentration $p < 3 \times 10^{20}\text{ cm}^{-3}$ the experiments indicate a spin-glass phase at temperatures below 0.5 K .^{9,10} However, at the temperatures we have performed our measurements ($T > 1.3\text{ K}$), these samples are paramagnetic and therefore we will call them paramagnetic throughout this article. The characteristic

threshold carrier concentration, $p_t = 3 \times 10^{20}\text{ cm}^{-3}$, observed in the studies of magnetic properties is also observed in transport and optical properties.^{4,11} It is equal to the total concentration of conducting holes necessary to occupy the second valence band of heavy holes [$E_F(p_t) = E_\Sigma$ in Fig. 1(a)]. The existence of ferromagnetism for low concentration of magnetic impurities ($x \geq 0.01$) and the dependence on the concentration of

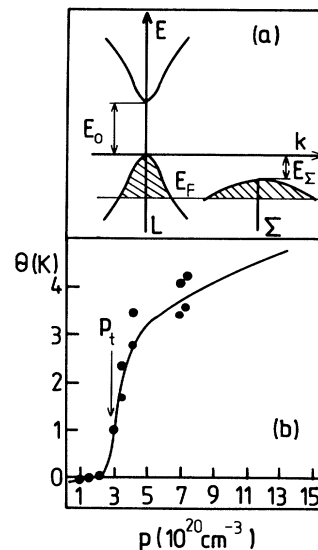


FIG. 1. (a) A simple model of the band structure of $\text{Pb}_{1-x-y}\text{Sn}_y\text{Mn}_x\text{Te}$. For samples with low carrier concentration only the band of light holes (L) is populated at low temperatures. The second valence band (Σ) is only populated for $p > p_t$ (Refs. 3-6). (b) Illustration of the carrier induced ferromagnetism in $\text{Pb}_{0.25}\text{Sn}_{0.72}\text{Mn}_{0.03}\text{Te}$ crystals. Points present the experimentally measured Curie temperatures. The solid line is the theoretical description based on the RKKY exchange interaction and the band-structure model (Ref. 12).

carriers strongly suggests that the ferromagnetic coupling between the spins of the magnetic ions is due to the Ruderman-Kittel-Kasuya-Yosida (RKKY) indirect exchange interaction via free holes. The presence of very heavy carriers from the Σ band leads to the strong enhancement of the RKKY interaction, which is directly proportional to the effective mass of carriers. Consequently, it generates the thresholdlike dependence of the Curie temperature on the concentration of carriers [Fig. 1(b)].¹² Increasing the carrier density even more ($p > 10^{21}$ cm⁻³) and for low manganese concentrations, a breakdown of the ferromagnetism to a spin-glass state has recently been found.¹³ This transition can be attributed to the intrinsic behavior of a RKKY-governed system.

The results of EPR studies of IV-VI diluted magnetic semiconductors so far may be summarized as follows. The investigations performed by Pifer on crystals of PbTe, PbSe, and PbS slightly doped with Mn, revealed a characteristic six line hyperfine pattern of Mn²⁺ ions.¹⁴ The g factor was found to be very close to 2.0 and the hyperfine constant $A_{\text{Mn}} = 61.2 \times 10^{-4}$ cm⁻¹. These observations were confirmed in more recent studies of crystals of PbTe:Mn,¹⁵⁻¹⁸ SnTe:Mn,¹⁹ GeTe:Mn,²⁰ and Pb_{1-x}Sn_xTe:Mn.²¹ It was also possible to observe the superhyperfine structure of the EPR line due to the interaction between the electronic spin of the Mn and the nuclear magnetic moment of Te ($A_{\text{Te}} = 15.4 \times 10^{-4}$ cm⁻¹).¹⁶⁻¹⁸ Due to the relatively strong hyperfine interaction, the observation of the cubic fine structure of the EPR signal of Mn²⁺ in IV-VI diluted magnetic semiconductors is obscured. However, in PbTe the cubic fine-structure constant was determined ($a = 36.5 \times 10^{-4}$ cm⁻¹) based on the analysis of the anisotropy of the EPR signal.¹⁷ With an increasing concentration of magnetic ions, the six line pattern is replaced by a single structureless line for $x > 0.002-0.004$. The EPR studies of these alloys were performed mostly on crystals of Pb_{1-x}Mn_xTe (Refs. 16 and 22) and Sn_{1-x}Mn_xTe (Refs. 23 and 24). The g factor was again found to be close to 2.0. The experimentally observed linear increase of the linewidth with an increasing temperature was interpreted based on the s - d exchange interaction between free carriers and localized spins (Korringa relaxation mechanism). In the case of Pb_{1-x}Mn_xTe the effect of electron bottleneck was found to influence the temperature dependence of the EPR linewidth.²² Based on the analysis of this temperature dependence the s - d exchange integral was determined: $J_{sd} = (70-80)$ meV (Refs. 15 and 16) for Pb_{1-x}Mn_xTe, with a carrier concentration ranging from $n = 1.2 \times 10^{18}$ cm⁻³ to $p = 5 \times 10^{19}$ cm⁻³ and $J_{sd} = 180$ meV for Sn_{1-x}Mn_xTe ($p = 4-8.5 \times 10^{20}$ cm⁻³).²³

As we quoted above, the magnetic behavior of these IV-VI systems, in which the J_{sd} interaction plays an important role, is sensitively related to the carrier concentration. In this paper therefore, we systematically explore effect of carrier concentration on the EPR linewidth, the s - d exchange interaction of holes with manganese spins and the low-temperature behavior of the linewidth and the resonance field in both paramagnetic and ferromagnetic samples. We will show that the strong increase of the linewidth with increasing temperature, ob-

served in the crystals of Sn_{1-x}Mn_xTe (Refs. 23 and 24) and Pb_{1-x-y}Sn_yMn_xTe (this work and Ref. 7), is strongly reduced for samples with carrier concentrations $p < p_i$. The effect can be interpreted based on the two-band model¹² of the magnetic properties of Pb_{1-x-y}Sn_yMn_xTe and the Korringa relaxation mechanism. We will show that earlier data, which seem contradictory in the appearance of the bottleneck effect, can be explained if the cation vacancies in the lattice are responsible for the electron-lattice relaxation. As the temperature is reduced ($T = 1.3-4.2$ K) an increase of the linewidth accompanied by a shift of the resonance field to lower fields is observed in all samples. In the case of ferromagnetic samples one observes a strong cubic anisotropy of the EPR resonance field and linewidth. Part of the experimental data presented in this paper was presented as a short communication in Ref. 25.

II. EXPERIMENTAL

A list of the samples of Pb_{1-x-y}Sn_yMn_xTe studied in this paper is presented in Table I. It covers the composition range $0.005 \leq x \leq 0.06$, $0.12 \leq y \leq 0.72$, and the carrier concentration range $p = 1.6 \times 10^{19} - 1.4 \times 10^{21}$ cm⁻³. The samples were grown by the Bridgman method. Most of them were checked by x-ray diffraction (Debye powder analysis and Laue method) and electron microprobe analysis. The crystals were found to be free of second phase inclusions and compositionally homogeneous. A typical value of the lattice constant is $a = 6.35$ Å (the sample with $x = 0.02$, $y = 0.72$, and $p = 5.5 \times 10^{20}$ cm⁻³). Laue patterns [usually for the (110) plane] characteristic for the rock salt structure were observed. It was observed that the pattern is twisted along an ingot. There was no change of this type within the cross section normal to the direction of crystal growth. Samples with different carrier concentrations were prepared by isothermal annealing in an atmosphere of tin (low-carrier-concentration samples) or tellurium (high-carrier-concentration samples).

Standard transport measurements (Hall effect and conductivity) were performed in the temperature range $T = 4.2-300$ K by an usual dc technique. Magnetization measurements were obtained in the temperature range $T = 1.5-20$ K using a vibrating sample magnetometer. The ac magnetic susceptibility was measured using a mutual inductance bridge. In all cases crystalline samples in the form of prolonged bars were used. EPR measurements were performed in the temperature range $T = 1.3-100$ K using an X-band spectrometer. Single structureless lines were observed in all the studied samples. Due to the high conductivity of the Pb_{1-x-y}Sn_yMn_xTe crystals (corresponding to a skin depth of about 7 μm) one observes a characteristic Dysonian shape of the line.^{26,27} To reduce this effect, the EPR investigations are frequently performed on powdered crystals. Most of the experiments in the present study were performed on samples both in the form of polished crystal plates (typical dimensions $7 \times 7 \times 1$ mm³) and powders immersed in an apiezon grease. In the first case the lineshape was very close to

TABLE I. Overview of the samples studied; FM: ferromagnetic, PM: paramagnetic, SG: spin glass.

Sample	Composition x	y	Carrier conc. $p [10^{20} \text{ cm}^{-3}]$	Curie temp. [K]	Low temp. magn. phase
A	0.005	0.72	5.1	?	?
B	0.01	0.72	6.9	≤ 2.0	FM
C	0.02	0.72	2.85	0.45	PM
D	0.02	0.72	5.5	2.7	FM
E	0.02	0.72	6.8	3.1	FM
F	0.02	0.72	14.0	3.8	SG
G	0.04	0.72	2.3	-0.4	PM
H	0.04	0.72	6.0	3.9	FM
I	0.02	0.12	0.16	-0.4	PM
J	0.04	0.16	0.17	-0.3	PM
K	0.06	0.16	0.61	-1.4	PM

the theoretical predictions. The resonance field (H_r) and the linewidth (ΔH) were determined by fits of the experimental spectra to the theory of Dyson. In the case of powdered samples the asymmetry of the line was reduced, but still present. In this case the peak to peak width (ΔH_{pp}) and half amplitude magnetic field of the experimental first derivative of the absorption signal was used to characterize the linewidth and the resonance field of the EPR spectrum.

III. EXPERIMENTAL RESULTS

Based on the results of the experimental investigations of the magnetic properties of our crystals, we can distinguish the following groups of samples. The samples with a carrier concentration *larger* than the threshold value $p_t = 3 \times 10^{20} \text{ cm}^{-3}$, but *smaller* than 10^{21} cm^{-3} are ferromagnetic at helium temperatures. A typical temperature dependence of the magnetic susceptibility of these samples is presented in Fig. 2. At high temperatures the magnetic susceptibility follows the Curie-Weiss law, with a positive (ferromagnetic) Curie temperature Θ (see also Fig. 1). The magnetic measurements on the sample *F*, with the *largest* carrier concentration revealed spin glass, rather than ferromagnetic properties.¹³ This is evidenced by the lack of characteristic critical behavior of the magnetic specific heat and the magnetic susceptibility (observed in all ferromagnetic samples). Instead, one observes a broad smooth magnetic contribution to the specific heat and a rather weak "cusplike" temperature dependence of the magnetic susceptibility. Samples with a carrier concentration *smaller* than the threshold value are all paramagnetic with a Curie temperature in the range $\Theta = 0 \pm 0.5 \text{ K}$. For samples with the lowest carrier concentrations ($p \ll p_t$), small negative (antiferromagnetic) values of Θ are observed. These experimental results are in full agreement with the model of magnetic properties of $\text{Pb}_{1-x-y}\text{Sn}_y\text{Mn}_x\text{Te}$ alloys¹² mentioned in the Introduction.

As expected^{1,2} we do not observe any temperature dependence of the carrier concentration in the temperature range $T \leq 100 \text{ K}$. The mobility, which is believed to be dominated by the impurity scattering mechanism, is

also very weakly temperature dependent in this temperature range.

The differences in magnetic properties of the samples of $\text{Pb}_{1-x-y}\text{Sn}_y\text{Mn}_x\text{Te}$ are primarily caused by the difference in carrier concentrations and are reflected in the results of EPR measurements presented below.

A. High-temperature region

A typical temperature dependence of the EPR linewidth of the samples with large carrier concentrations ($p > p_t$) is presented in Fig. 3 (solid symbols). The strong

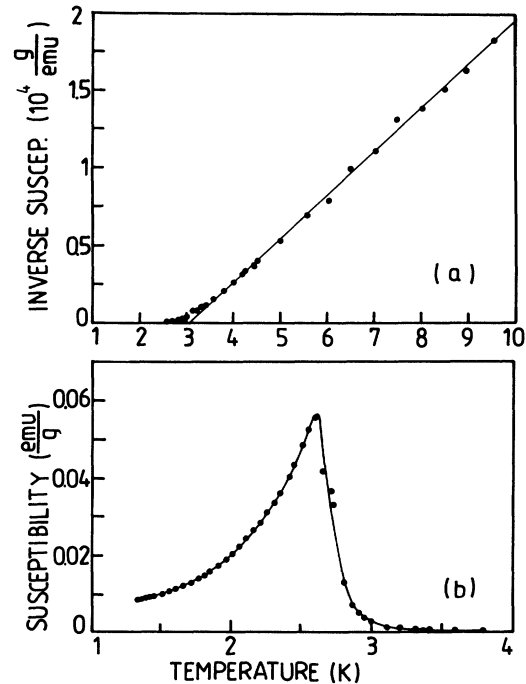


FIG. 2. (a) The temperature dependence of the inverse magnetic susceptibility of the sample $\text{Pb}_{0.26}\text{Sn}_{0.72}\text{Mn}_{0.02}\text{Te}$ with carrier concentration $p = 6.8 \times 10^{20} \text{ cm}^{-3}$ at temperatures $T > \Theta$. (b) The temperature dependence of the ac magnetic susceptibility in the transition temperature region ($T < \Theta$).

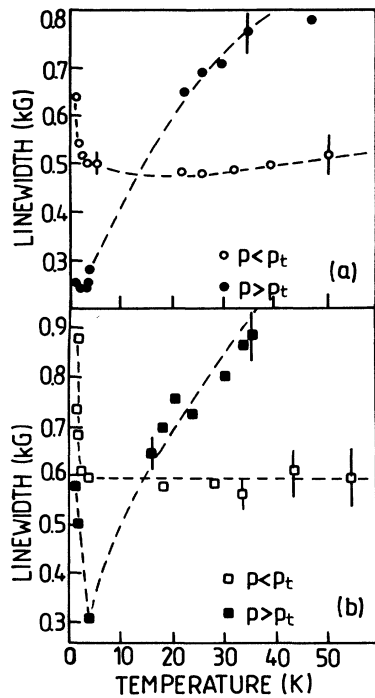


FIG. 3. Temperature dependence of the EPR linewidth. (a) crystalline plates with $x=0.02$, $y=0.72$, and $p=5.5 \times 10^{20} \text{ cm}^{-3}$ (solid circles) and $p=2.85 \times 10^{20} \text{ cm}^{-3}$ (open circles). (b) powdered samples with $x=0.04$, $y=0.72$, and $p=6.0 \times 10^{20} \text{ cm}^{-3}$ (solid squares) and $p=2.3 \times 10^{20} \text{ cm}^{-3}$ (open squares).

increase of the linewidth with temperature is observed for all manganese concentrations in both crystalline [Fig. 3(a)] and powdered samples [Fig. 3(b)]. The fast broadening of the line leads to the complete disappearance of the EPR signal at temperatures $T \geq 50\text{--}70 \text{ K}$. Within the experimental accuracy, there is no temperature dependence

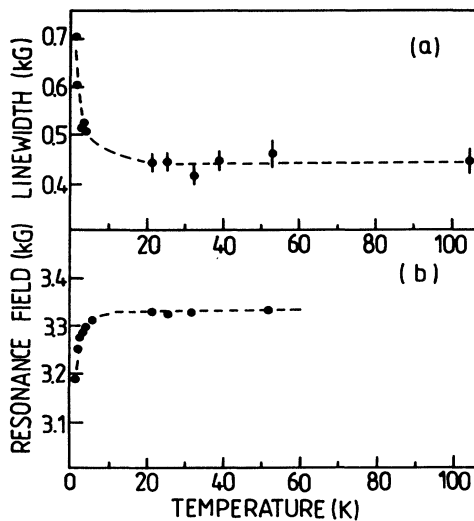


FIG. 4. Temperature dependence of the linewidth and resonance field of $\text{Pb}_{0.80}\text{Sn}_{0.16}\text{Mn}_{0.04}\text{Te}$ with low carrier concentration $p = 1.7 \times 10^{19} \text{ cm}^{-3} \ll p_t$.

of the EPR resonance field. The observed resonance corresponds to $g=2.0$.

Even a small reduction of carrier concentration below the threshold value changes the temperature dependence of the EPR linewidth significantly (open symbols in Fig. 3). The temperature dependence in this case is very weak. Again we do not observe a temperature dependence of the resonance field at $g=2.0$.

The reduction of the temperature dependence of the linewidth is even stronger in the case of samples with the lowest carrier concentrations (Fig. 4), where there is practically no temperature dependence of the EPR signal in the high-temperature region. One has to notice, however, that in this high-temperature region, due to the relatively broad lines and limited temperature range in which they are observed, we are unable to detect a possible weak temperature dependent contribution to the linewidth. This also significantly decreases the precision of the determination of the resonance field.

B. Low-temperature region

A typical behavior of the EPR linewidth and the resonance field of the paramagnetic samples $\text{Pb}_{1-x-y}\text{Sn}_y\text{Mn}_x\text{Te}$ ($p < p_t$) at low temperatures is presented in Figs. 4 and 5. With a decreasing temperature an increase of the EPR linewidth is observed [Fig. 5(a)]. It is accompanied by a shift of the resonance field to lower fields [Fig. 5(b)]. The effect is observed both in powdered crystals and crystalline plates. In the latter case the experimental investigations were performed in two configurations, i.e., the surface of the sample parallel and normal to the external magnetic field. The shift of the resonance field is observed in both configurations.

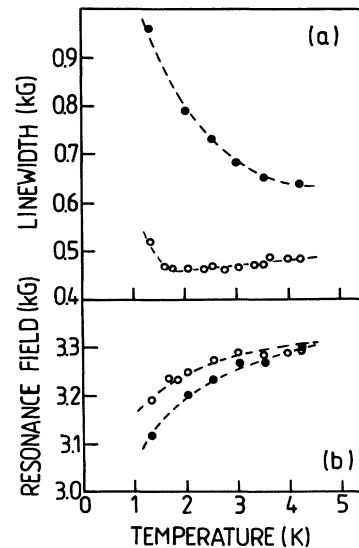


FIG. 5. EPR linewidth and resonance field vs temperature (at low temperatures) for two powdered samples with carrier concentration lower than the threshold value. Open circles: $x=0.02$, $y=0.72$, and $p=2.85 \times 10^{20} \text{ cm}^{-3}$; solid circles: $x=0.04$, $y=0.72$, and $p=2.3 \times 10^{20} \text{ cm}^{-3}$.

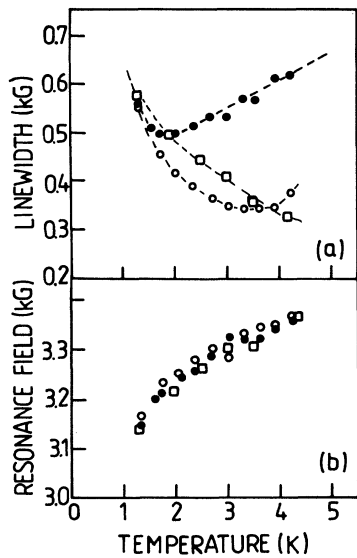


FIG. 6. Temperature dependence of the linewidth and the resonance field of powdered samples with different manganese concentrations. Solid circles: $x=0.01$, $y=0.72$, and $p=6.9 \times 10^{20} \text{ cm}^{-3}$; open circles: $x=0.02$, $y=0.72$, and $p=5.5 \times 10^{20} \text{ cm}^{-3}$; open squares: $x=0.04$, $y=0.72$, and $p=6.0 \times 10^{20} \text{ cm}^{-3}$.

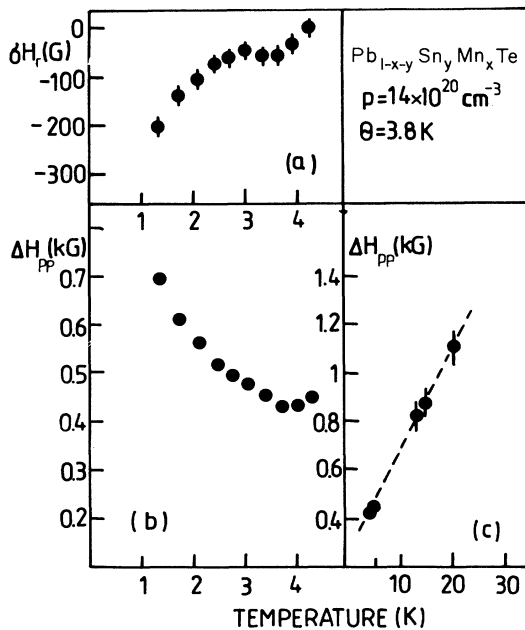


FIG. 7. Temperature dependence of the resonance field and the linewidth of the sample of $\text{Pb}_{0.26}\text{Sn}_{0.72}\text{Mn}_{0.02}\text{Te}$ with the largest carrier concentration $p=1.4 \times 10^{21} \text{ cm}^{-3}$, a spin glass at $T \approx 1.5 \text{ K}$, with $\Theta=3.8 \text{ K}$. (a) shift of the resonance field $\delta H_r(T) = H_r(T) - H_r(4.2 \text{ K})$; (b) and (c) linewidth at low and high temperatures.

This excludes the demagnetization fields as a primary source of this effect. We observed the same characteristic behavior in all paramagnetic samples. The magnitude of the effect is manganese concentration dependent (Fig. 5).

Our samples, which exhibit a ferromagnetic phase transition at low temperatures, show a dramatic increase of the intensity of the EPR signal at these temperatures. All these samples have a carrier concentration larger than the threshold concentration. The temperature dependence of the resonance field and the linewidth are presented in Fig. 6 for three powdered samples with different manganese concentrations. The linewidth has a minimum at a temperature approximately equal to the Curie temperature of the crystal. The shift of H_r to lower fields is manganese concentration independent.

EPR measurements on sample F which, according to magnetic measurements is a spin glass at low temperatures, are presented in Fig. 7. As for all other samples with a carrier concentration $p > p_t$, the linewidth at high temperatures is increasing very fast with increasing temperature [Fig. 7(c)]. At low temperatures a particularly strong increase of the linewidth [Fig. 7(b)] and the shift of the resonance field [Fig. 7(a)] are observed. The EPR resonance field is anisotropic at $T < \Theta$.

IV. DISCUSSION

A schematic overview of the results is presented in Fig. 8. Each temperature and carrier-concentration range is characterized by a typical temperature dependence of the EPR linewidth and the resonance field at low ($T < \Theta$) and high ($T > \Theta$) temperatures. The threshold concentration of carriers, $p_t = 3 \times 10^{20} \text{ cm}^{-3}$ presents a clear dis-

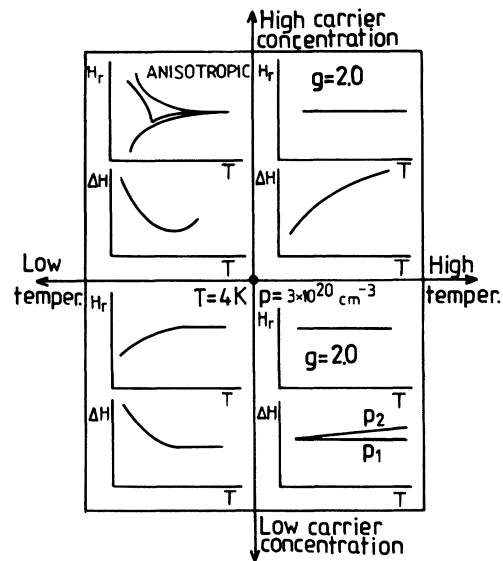


FIG. 8. A schematic overview of the temperature and carrier concentration dependence of the EPR linewidth (ΔH) and the resonance field (H_r) of crystals of $\text{Pb}_{1-x-y}\text{Sn}_y\text{Mn}_x\text{Te}$. In the manganese concentration range studied $0.005 \leq x \leq 0.06$ there is no qualitative effect of the concentration of manganese ions on EPR.

tion in general behavior, while the transition from low-temperature to high-temperature behavior is located somewhere in the liquid-helium range. We will discuss the experimental results in these two temperature ranges separately.

A. High-temperature region

Before discussing the linewidth, we would like to note that all the experimental data accumulated so far (including the present work) support the concept of manganese incorporated into the matrix of IV-VI semiconductors as a Mn^{2+} ion with spin-only magnetic moment $S=5/2$. Because spin-orbit coupling is involved in the spin-lattice relaxation, and $L=0$, the spin-lattice relaxation is expected to be very inefficient and far too slow to account for the observed EPR linewidths.²⁸⁻³⁰ The most important effects observed in this temperature range are the rapid increase of the linewidth with an increasing temperature observed in all samples with a carrier concentration exceeding the threshold value, as well as the sudden discontinuity of this effect at $p=p_t$ [see Fig. 9(a)]. The increase of the linewidth with temperature is similar to the behavior in the closely related system $\text{Sn}_{1-x}\text{Mn}_x\text{Te}$,^{23,24} and the samples of $\text{Pb}_{0.25}\text{Sn}_{0.72}\text{Mn}_{0.03}\text{Te}$,⁷ where it is usually attributed to the Korringa relaxation mechanism. This mechanism, which originates from the s - d exchange interaction between carriers and localized spins, is expected to be effective in $\text{Pb}_{1-x-y}\text{Sn}_y\text{Mn}_x\text{Te}$ crystals with a high concentration of carriers. The discontinuity at p_t confirms the important role of the carriers in the linewidth broadening mechanism.

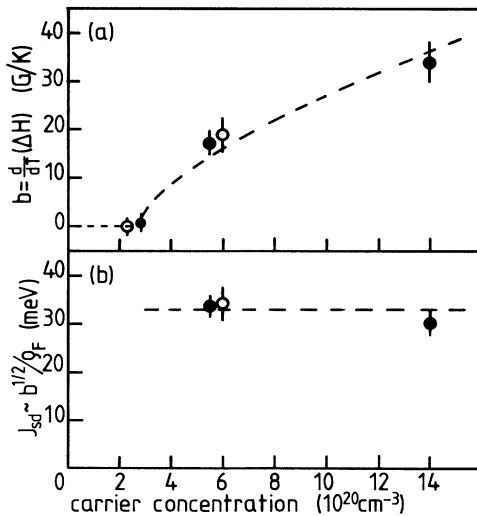


FIG. 9. (a) The carrier concentration dependence of the Korringa slope $b = (\pi/\hbar)J_{sd}^2(\rho_F/N)^2k_B$. The experimental points were obtained for the samples with composition $x=0.02$, $y=0.72$ (solid symbols) and $x=0.04$, $y=0.72$ (open symbols). The sudden increase of the slope for $p > p_t$ is due to the increase of the density of states in the band of heavy holes. (b) The same experimental points rescaled according to the expression 1.

Microscopically, the Korringa mechanism represents a relaxation of the magnetic system to the conduction carriers, which is of primary importance for EPR of local magnetic moments in metallic hosts.^{31,32} The relaxation rate for this mechanism (δ_{Me}) is given by

$$\delta_{\text{Me}} = \frac{1}{\tau_{\text{Me}}} = \frac{\pi}{\hbar} J_{sd}^2 \left(\frac{\rho_F}{N} \right)^2 k_B T, \quad (1)$$

where J_{sd} is the exchange integral, ρ_F is the density of states at the Fermi level, and N is the number of lattice points per unit volume. The contribution to the EPR linewidth is proportional to the relaxation rate

$$\Delta H = \frac{\hbar}{g\mu_B} \delta_{\text{Me}}. \quad (2)$$

When the spin relaxation is dominated by the Korringa mechanism, one expects a linear temperature dependence of the linewidth. In real systems^{31,32} the EPR linewidth is at low temperatures determined by temperature independent processes of inhomogeneous broadening due to, e.g., dipole-dipole interaction. Therefore, in many metallic systems, the temperature dependence of the linewidth can be described by the simple expression

$$\Delta H = a + bT, \quad (3)$$

where a is the residual width and bT is the Korringa contribution. The analysis of the Korringa mechanism in the case of a system of interacting spins (the situation encountered in our samples) showed that the linewidth in the paramagnetic phase may still be described with Eq. (3). In this case the residual width depends on the strength of the d - d interspin interaction as monitored by the paramagnetic Curie temperature (Ref. 33). The slope b is a measure of the exchange integral J_{sd} .

As quoted already the Korringa relaxation mechanism was proposed as an origin of the temperature dependence of the EPR linewidth in $\text{Sn}_{1-x}\text{Mn}_x\text{Te}$ (Refs. 23 and 24) and $\text{Pb}_{1-x}\text{Mn}_x\text{Te}$ (Refs. 15, 16, and 22). It was also found important in one of the II-IV diluted magnetic semiconductors, namely HgSe:Fe .³⁴

Within the framework of the Korringa relaxation mechanism, the dramatic difference of the temperature dependence of the linewidth observed in samples with a carrier concentration below and above the threshold concentration can be understood on the basis of the two-valence-band model¹² of magnetic properties of $\text{Pb}_{1-x-y}\text{Sn}_y\text{Mn}_x\text{Te}$ crystals. The Korringa relaxation rate depends on the density of states at the Fermi level. The large difference between the densities of states associated with the band of light holes (populated for $p < p_t$) and the band of heavy holes (populated only for $p > p_t$), explains the strong enhancement of the Korringa mechanism in samples with $p > p_t$. In the case of samples with $p < p_t$ only light holes contribute to the Korringa mechanism. Due to the small density of states in the L band, this contribution can be smaller than the residual linewidth, which results in a very weak temperature dependence of the linewidth as observed in these samples.

In the samples with $p > p_t$ the density of states is much

higher, which results in a stronger temperature dependence of the linewidth. In our calculation of J_{sd} we have assumed the second valence band to be parabolic and twofold degenerate,³⁵ and the (small) contribution of the carriers from the L band has been neglected. Using the relations 1 and 2 we have obtained $J_{sd} = 33 \pm 2$ meV. The value of J_{sd} in the range $p > p_t$ turned out to be independent of the carrier concentration and manganese content [see Fig. 9(b)]. Compared to the values of J_{sd} mentioned in Sec. I, the present value of J_{sd} is lower than for $\text{Pb}_{1-x}\text{Mn}_x\text{Te}$. However, these values were obtained in low-carrier-concentration material, in which only the L band plays a role. This seems to indicate that the s - d exchange interaction for the L band is larger than the value for the Σ band. The value of J_{sd} given by Cochrane, Hedgcock, and Lightstone²³ (180 meV), obtained in the restricted carrier-concentration regime $p = (4-8) \times 10^{20} \text{ cm}^{-3}$, is based on a different interpretation of the results. When we review their measurements and interpret those with the same band-structure parameters we used, a value of $J_{sd} = 31 \pm 4$ meV is obtained, in perfect agreement with our analysis. Finally we would like to stress that measurements of the Curie-Weiss temperature could be explained using $J_{sd} = 100$ meV.⁴ This discrepancy may be attributed to the wave vector dependence of the exchange integral as was observed before,³⁶ but also uncertainties in other parameters, determining the strength of the prevailing RKKY mechanism might be responsible for the difference.

The analysis described above is only applicable if the Korringa relaxation is the only relaxation process of importance. Usually the analysis is based on the Bloch-Hasegawa equations.³¹⁻³³ These are two equations describing the dynamics of two distinct spin subsystems: The system of local magnetic moments (with g factor g_M) and the system of conducting carriers (g factor g_e).

$$\frac{d\mathbf{M}_M}{dt} = g_M \mu_B \mathbf{M}_M \times (\mathbf{H}_{\text{ext}} + \lambda \mathbf{M}_e) - (\delta_{M_e} + \delta_{M_L}) \delta \mathbf{M}_M + \delta_{eM} \frac{g_M}{g_e} \delta \mathbf{M}_e, \quad (4a)$$

$$\frac{d\mathbf{M}_e}{dt} = g_e \mu_B \mathbf{M}_e \times (\mathbf{H}_{\text{ext}} + \lambda \mathbf{M}_M) - (\delta_{eL} + \delta_{eM}) \delta \mathbf{M}_e + \delta_{M_e} \frac{g_e}{g_M} \delta \mathbf{M}_M, \quad (4b)$$

where $\delta \mathbf{M}_M$ and $\delta \mathbf{M}_e$ are the deviations of \mathbf{M}_M and \mathbf{M}_e respectively from the local equilibrium magnetization. The usual Bloch equations are here supplemented with additional relaxation terms. The transfer of magnetic moment from local moments to conducting carriers is described by the Korringa mechanism [δ_{M_e} , Eq. (1)]. The backflow of magnetization from carriers to local moments is described by the Overhauser (δ_{eM}) mechanism, with

$$\delta_{eM} = \frac{1}{\tau_{eM}} = \frac{2\pi}{3\hbar} J_{sd}^2 \left[\frac{\rho_F}{N} \right] x S(S+1). \quad (5)$$

The electron-lattice relaxation rate is given by

$$\delta_{eL} = \frac{16\pi c_d}{9\hbar} \frac{\rho_F}{N} |V_{so}|^2, \quad (6)$$

where c_d is the concentration of defects effective in spin relaxation and V_{so} is the scattering potential. All these spin-relaxation channels are illustrated in Fig. 10.

The theoretical analysis of the Bloch-Hasegawa equations shows that the simple expression (1) is only valid under, so called, nonbottlenecked resonance conditions. Under these conditions the energy transferred from the system of local moments is further transferred to the crystal lattice (defects or phonons), with a relatively high relaxation rate, i.e., $\delta_{eL} > \delta_{eM}$. In many real systems this condition is not satisfied, and there is a considerable backflow of energy from carriers to local moments. Under such (electron bottleneck) conditions the experimentally observed slope b [Eq. (3)] is reduced by the factor $\delta_{eL}/(\delta_{eL} + \delta_{eM})$.³⁷ So, the understanding of the bottleneck effect is important for a proper analysis of the exchange constant based on the EPR data. Experimentally, the presence of the bottleneck effect can be evidenced by the fact that the b in Eq. (3) is magnetic impurity concentration dependent. For bottlenecked resonance one expects $b \propto 1/x$, whereas for nonbottlenecked resonance b is magnetic impurity concentration independent.

The experimental data about the bottleneck effect in IV-VI diluted magnetic semiconductors accomplished so far are following. In crystals of $\text{Sn}_{1-x}\text{Mn}_x\text{Te}$ the Korringa slope was found to be manganese concentration independent within the wide concentration range $0.002 \leq x \leq 0.1$ [23], which indicates the nonbottlenecked character of the resonance. Rather contradictory results were observed for $\text{Pb}_{1-x}\text{Mn}_x\text{Te}$. No bottleneck was found in crystals with composition $0.00015 \leq x \leq 0.003$.¹⁵ However, it was found important in crystals with compositions $0.006 \leq x \leq 0.03$ (Ref. 22) and $0.009 \leq x \leq 0.0172$ (Ref. 16). Our experimental data for $\text{Pb}_{1-x-y}\text{Sn}_y\text{Mn}_x\text{Te}$ crystals indicate no manganese concentration dependence of the temperature dependence of the linewidth for samples with $p > p_t$. This suggests that EPR is not bottlenecked in these alloys and we are allowed to use the

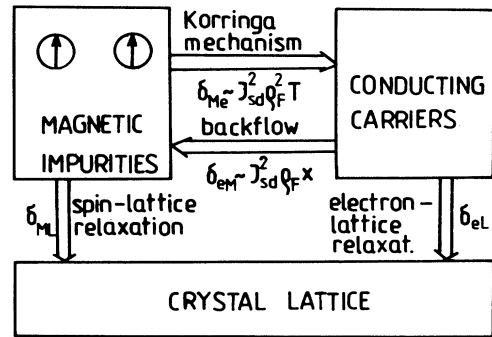


FIG. 10. Diagram of the spin-relaxation mechanisms relevant in an analysis of EPR of localized magnetic impurities in metallic matrices. (After Refs. 31 and 32.)

simple expression (1) to evaluate the exchange integral. The experimental data for samples with $p < p_t$ are not conclusive. The very weak temperature dependence of the linewidth is mainly caused by the relatively small Korringa contribution to the linewidth. The Korringa mechanism may also be additionally suppressed by the bottleneck effect as we will discuss below.

One may attempt to explain all these experimental observations related to the bottleneck effect IV-VI diluted magnetic semiconductors within the following simple model. The bottleneck effect is important in the case when the transfer of energy from conducting carriers to the lattice is not fast enough to prevent the backflow relaxation to the local moments system, i.e., $\delta_{eL} < \delta_{eM}$. Let us assume that vacancies, the main defects in IV-VI alloys (generating conducting carriers), are the scattering centers responsible for the spin-lattice relaxation of carriers. In such a case the concentration of scattering centers is proportional to the concentration of carriers $c_d \propto p$. One can see [Eqs. (1) and (6)] that with increasing concentration of carriers (i.e., also the concentration of scattering centers) the electron-lattice relaxation is increasing faster than the electron-local moments relaxation. In the parabolic band approximation:

$$\delta_{eL} \propto V_{so}^2 p^{4/3}, \quad \text{and} \quad \delta_{eM} \propto J_{sd}^2 p^{1/3} x. \quad (7)$$

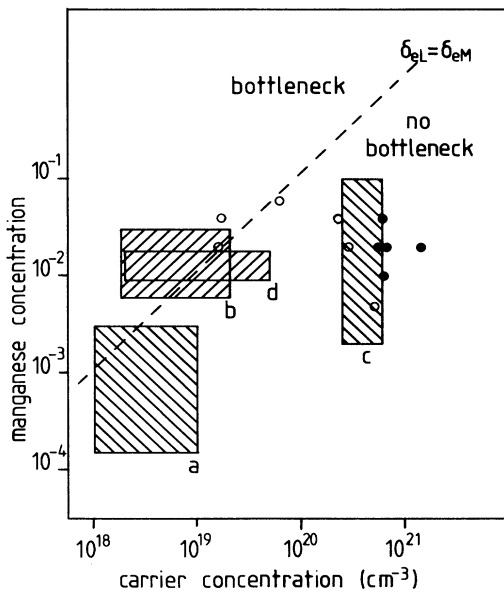


FIG. 11. A proposed interpretation of the role of the bottleneck effect in the EPR of Mn^{2+} in IV-VI semiconductors. Left hatched boxes indicate regions in which no bottleneck is found, right hatched boxes show regions where a bottleneck is found. Solid circles are samples from this work in which no bottleneck is found, open circles are samples from this work for which the measurements were not conclusive about bottleneck conditions. The dashed line indicates $\delta_{eL} = \delta_{eM}$, which is the boundary between the two regimes. This line is drawn based upon the data presented here. (a) Ref. 15, (b) Ref. 22, (c) Ref. 23, and (d) Ref. 16.

Based on this hypothesis one can see that the bottleneck effect is not expected to be important for samples with large carrier concentration. The bottleneck effect may play a role in low-carrier-concentration samples with a relatively high manganese content. These are the crystals in which the bottleneck effect was really observed in PbMnTe .^{16,22} In more diluted samples with bottleneck effect is not important in both low- and high-carrier-concentration samples.¹⁵ The role of the bottleneck effect in IV-VI alloys based on this hypothesis is illustrated in Fig. 11. The line separating bottlenecked and non-bottlenecked regions in the (x, p) plane is determined by the condition $\delta_{eL} = \delta_{eM}$, i.e., $(p/x) = \text{const}$. It is fixed in this plane based on the experimental observations of Tatsukawa²² and Korczak¹⁶ that the EPR of Mn in PbTe is bottlenecked for samples with $x = 0.006 - 0.03$ and $p = (0.5 - 5) \times 10^{19} \text{ cm}^{-3}$.

B. Low-temperature region

At low temperatures we expect the Korringa mechanism contribution to the EPR linewidth to be small. The linewidth is not governed by the spin-relaxation processes but it is determined by inhomogeneous broadening. In crystals in which there is a considerable interspin exchange interaction between magnetic moments, the mechanism of exchange narrowing is also expected to be important. Experimentally, one observes a typical linewidth of $\Delta H \approx 400 - 500 \text{ G}$ in paramagnetic samples. This is about the value expected, based on the dipole-dipole broadening of the hyperfine structure of the EPR line.³⁸

In all the samples with a low carrier concentration, we observe qualitatively the same temperature behavior of the linewidth and the resonance field. With a decreasing temperature, the linewidth is increasing and the resonance field is shifting to lower fields. In all samples with $p > p_t$ (ferromagnetic at low temperatures) a strong anisotropy in the resonance field is observed, which will be discussed below. The average behavior (as measured on powders) is similar to the behavior in the low-carrier-concentration regime, although much stronger. The same type of behavior was also found in the case of the spin-glass sample F.

The temperature dependence of the resonance field and the linewidth described above is qualitatively similar to the behavior found in numerous magnetic systems.^{30-34,39,40} It is usually attributed to the effect of the $d-d$ exchange interaction (RKKY interaction in our case) resulting in the formation of magnetic order at low temperatures. The increase of the linewidth is caused by the slowing down of the fluctuations of the magnetization of the local moments system due to spin correlations present at temperatures $T \leq \Theta$. It reduces the efficiency of the exchange narrowing, thereby contributing to the temperature dependence of the EPR linewidth. The shift of the resonance field results from the presence of the additional (molecular) field acting on spins that increases with decreasing temperature (increasing magnetization). This interpretation of the temperature dependence of the resonance field and the linewidth is probably valid in the case

of our samples with $p > p_t$ for which there is a relatively strong RKKY exchange interaction. This is also evidenced by the correlation of the Curie temperature and the minimum in the temperature dependence of the linewidth.

In the case of the samples with $p < p_t$ there is no phase transition in the temperature range studied $T \geq 1.3$ K. The d - d exchange interaction is rather weak. One should probably exclude the mechanism described above as relevant in this case. It follows also from the apparent lack of correlation between the Curie temperature and the plot of $\Delta H(T)$. In this case one can consider an other mechanism influencing the linewidth, which was proposed in Refs. 16 and 37. According to this mechanism, the increase of the linewidth with decreasing temperature is caused by the temperature dependent narrowing of the inhomogeneously broadened line. The narrowing mechanism originates from the cross relaxation under bottleneck conditions. As follows from our discussion, one can expect the bottleneck effect to be important in low-carrier-concentration samples. One can also expect that the line is inhomogeneously broadened at low temperatures.³⁷

V. CONCLUSIONS

We observed the electron paramagnetic resonance of manganese ions in $\text{Pb}_{1-x-y}\text{Sn}_y\text{Mn}_x\text{Te}$. At high temper-

atures, the g factor is close to 2.0 in all samples, irrespective of their low-temperature magnetic behavior. This supports the idea that the Mn ions are in a spin-only state.

The threshold carrier concentration $p_t = 3 \times 10^{20} \text{ cm}^{-3}$, previously observed in magnetization and ac susceptibility measurements, is also evident in EPR measurements. For samples with $p > p_t$ there is a strong increase of the linewidth with increasing temperature, yielding an exchange integral for the heavy holes of $J_{sd} = 33 \pm 2 \text{ meV}$. For samples with $p < p_t$ there is only a very weak temperature dependence of the linewidth. We have shown that this can be described with a model based on the Korringa relaxation mechanism and the two-valence-band model of magnetic properties of $\text{Pb}_{1-x-y}\text{Sn}_y\text{Mn}_x\text{Te}$. We also discussed the conditions under which the bottleneck effect may influence the EPR of Mn ions in IV-VI alloys with a special emphasis on the role of metal vacancies.

ACKNOWLEDGMENTS

We would like to thank Professor R. R. Gałazka and Dr. K. Kopinga for helpful discussions and J. H. J. Daldrop, E. Grodzicka, A. Jędrzejczak, M. Leszczyński, and C. van der Steen for help during the measurements and the characterization of our samples. The research of Dr. Swagten is made possible by financial support from the Royal Netherlands Academy of Arts and Sciences.

*On leave from the Institute of Physics, Polish Academy of Sciences, Al. Lotników 32/46, 02-668 Warsaw, Poland.

- ¹R. R. Gałazka, in *Proceedings of the 14th International Conference on the Physics of Semiconductors, Edinburgh, 1978*, edited by B. L. H. Wilson, IOP Conf. Proc. No. 43 (Institute of Physics and Physical Society, London, 1978); G. Bauer, in *Diluted Magnetic Semiconductors*, edited by R. L. Aggarwal, J. K. Furdyna, and S. von Molnar, MRS Symposia Proceedings No. 89 (Materials Research Society, Pittsburgh, 1987); J. K. Furdyna, *J. Appl. Phys.* **64**, R29 (1988); W. J. M. de Jonge and H. J. M. Swagten, *J. Magn. Magn. Mater.* **100**, 322 (1991).
- ²G. Nimtz, and B. Schlicht, in *Narrow Gap Semiconductors*, edited by G. Höhler and E. A. Niekisch, Springer Tracts in Modern Physics, Vol. 98 (Springer, Berlin, 1983).
- ³T. Story, R. R. Gałazka, R. B. Frankel, and P. A. Wolff, *Phys. Rev. Lett.* **56**, 777 (1986).
- ⁴T. Story, G. Karczewski, L. Swierkowski, and R. R. Gałazka, *Phys. Rev. B* **42**, 10 477 (1990).
- ⁵T. Story, G. Karczewski, L. Swierkowski, M. Górska, and R. R. Gałazka, *Semicond. Sci. Technol.* **5**, S138 (1990).
- ⁶W. J. M. de Jonge, H. J. M. Swagten, S. J. E. A. Eltink and N. M. J. Stoffels, *Semicond. Sci. Technol.* **5**, S131 (1990).
- ⁷M. Z. Cieplak, A. Sienkiewicz, Z. Wilamowski, and T. Story, *Acta Phys. Pol. A* **69**, 1011 (1986).
- ⁸C. W. H. M. Vennix, E. Frikkee, H. J. M. Swagten, K. Kopinga, and W. J. M. de Jonge, *J. Appl. Phys.* **69**, 6025 (1991).
- ⁹H. J. M. Swagten, H. van de Hoek, W. J. M. de Jonge, R. R. Gałazka, P. Warmenbol, and J. T. Devreese, in *Proceedings of the 19th International Conference on the Physics of Semiconductors, Warsaw, 1988*, edited by W. Zawadzki (Institute of Physics, Polish Academy of Sciences, Warsaw, 1988) p. 1559.

- ¹⁰F. T. Hedgcock, P. C. Sullivan, K. Kadowaki, and S. B. Woods, *J. Magn. Magn. Mater.* **54-57**, 1293 (1986).
- ¹¹G. Karczewski, L. Swierkowski, T. Story, A. Szczerbakow, J. Niewodniczańska-Blinowska, and G. Bauer, *Semicond. Sci. Technol.* **5**, 1115 (1990).
- ¹²H. J. M. Swagten, W. J. M. de Jonge, R. R. Gałazka, P. Warmenbol, and J. T. Devreese, *Phys. Rev. B* **37**, 9907 (1988).
- ¹³W. J. M. de Jonge, T. Story, H. J. M. Swagten, and P. J. T. Eggenkamp, *Europhys. Lett.* **17** 631 (1992).
- ¹⁴J. H. Pifer, *Phys. Rev.* **157**, 272 (1967).
- ¹⁵G. Toth, J. Y. Leloup, and H. Rodot, *Phys. Rev. B* **1**, 4573 (1970).
- ¹⁶S. Z. Korczak, W. Korczak, M. Subotowicz, and H. Wasiewicz, *Phys. Status Solidi B* **153**, 361 (1989).
- ¹⁷H. Lettenmayr, W. Jantsch, and L. Palmetshofer, *Solid State Commun.* **64**, 1253 (1987).
- ¹⁸M. Bartkowski, D. J. Northcott, and A. H. Reddoch, *Phys. Rev. B* **34**, 6506 (1986).
- ¹⁹M. Inoue, H. Yagi, T. Muratani, and T. Tatsukawa, *J. Phys. Soc. Jpn.* **40**, 458 (1976).
- ²⁰M. Inoue, Y. Kaku, H. Yagi, and T. Tatsukawa, *J. Phys. Soc. Jpn.* **43**, 512 (1977).
- ²¹M. Inoue, H. Yagi, T. Tatsukawa, and Y. Kaku, *J. Phys. Soc. Jpn.* **45**, 1610 (1978).
- ²²T. Tatsukawa, *J. Phys. Soc. Jpn.* **50**, 515 (1981).
- ²³R. W. Cochrane, F. T. Hedgcock, and A. W. Lightstone, *Can. J. Phys.* **56**, 68 (1978); R. W. Cochrane, F. T. Hedgcock, and A. W. Lightstone, in *Proceedings of the 14th International Conference on Low Temperature Physics, Otaniemi, Finland, 1975*, edited by M. Krusius and M. Vuorio (North-Holland, Amsterdam, 1975), Vol. 3, p. 290.
- ²⁴P. Urban and G. Sperlich, *Solid State Commun.* **16**, 927

- (1975).
- ²⁵T. Story, C. H. W. Swüste, H. J. M. Swagten, R. J. T. van Kempen, and W. J. M. de Jonge, *J. Appl. Phys.* **69**, 6037 (1991).
- ²⁶F. J. Dyson, *Phys. Rev.* **98**, 349 (1955).
- ²⁷J. Owen, M. B. Browne, V. Arp, and A. F. Kip, *J. Phys. Chem. Solids* **2**, 85 (1957); J. Owen, M. Browne, W. D. Knight, and C. Kittel, *Phys. Rev.* **102**, 1501 (1956).
- ²⁸J. H. Van Vleck, *Phys. Rev.* **57**, 426 (1940).
- ²⁹K. W. H. Stevens, *Rep. Prog. Phys.* **30**, 189 (1967).
- ³⁰A. Abragam and B. Bleaney, *Electron Paramagnetic Resonance of Transition Ions* (Clarendon, Oxford, 1970).
- ³¹S. E. Barnes, *Adv. Phys.* **30**, 801 (1981).
- ³²R. H. Taylor, *Adv. Phys.* **24**, 681 (1975).
- ³³S. E. Barnes, *Phys. Rev. B* **30**, 3944 (1984).
- ³⁴Z. Wilamowski, A. Mycielski, W. Jantsch, and G. Hendorfer, *Phys. Rev. B* **38**, 3621 (1988).
- ³⁵T. Story, P. J. T. Eggenkamp, C. H. W. Swüste, H. J. M. Swagten, W. J. M. de Jonge, and L. F. Lemmens, *Phys. Rev. B* **45**, 1660 (1992).
- ³⁶D. Davidov, K. Maki, R. Orbach, C. Rettori, and E. P. Chock, *Solid State Commun.* **12**, 621 (1973).
- ³⁷L. P. Tagirov and K. F. Trutnev, *Zh. Eksp. Teor. Fiz.* **86**, 1092 (1984) [*Sov. Phys. JETP* **59**, 638 (1984)].
- ³⁸J. H. Van Vleck, *Phys. Rev.* **74**, 1168 (1948).
- ³⁹M. Zomack, K. Baberschke, and S. E. Barnes, *Phys. Rev. B* **27**, 4135 (1983).
- ⁴⁰G. Mozurkewicz, J. H. Elliott, M. Hardiman, and R. Orbach, *Phys. Rev. B* **29**, 278 (1984).